14th Australasian Fluid Mechanics Conference
Adelaide University, Adelaide, Australia
10-14 December 2001

Finite Element Modeling of Generalised Newtonian Flows

W. Barth[1], G. Carey[1], S. Chow[2], B. Kirk[1]

[1]Aerospace Engineering Department
The University of Texas at Austin, Austin, Texas, 78712 USA

[2]Department of Mathematics
Brigham Young University, Salt Lake City, Utah 99999 USA

Abstract

Here we consider finite element modeling of coupled flow and heat transfer for Eyring-Powell and Williamson generalized viscosity models. Supporting numerical studies are provided using a domain-decomposition approach for simulations on a Beowulf cluster.

Introduction

In this study we describe finite element research for coupled fluid flow and transport applications. Of particular interest are incompressible viscous Newtonian and generalized Newtonian flows with the Boussinesq assumption and where thermocapillary surface tension effects may be important at a free surface. Applications in both two and three dimensions are considered for a Galerkin primitive variable formulation using C^0 tensor product bases.

The implementation for both steady and transient simulations involves domain decomposition with non-overlapping grid cells and shared nodes on the interfaces of adjacent subdomains. Parallel algorithms have been developed within this setting that use Krylov subspace iteration with element-by-element calculations within processors assigned to subdomains and communication between processors at the subdomain boundaries.

The approach is applied for phenomenological studies of natural convection and similar problems on distributed parallel supercomputers and on Beowulf PC cluster architectures. Results of applications to Newtonian, Eyring-Powell and Williamson generalized Newtonian fluid models as well as parallel performance studies are provided.

Governing PDE System

Consider the problem of flow of heated incompressible viscous fluid given by

$$\rho(\frac{\partial \boldsymbol{u}}{\partial t} + \boldsymbol{u}\cdot\nabla\boldsymbol{u}) + \nabla\cdot\boldsymbol{\tau} = \boldsymbol{f} - \rho\beta(T-T^*)\boldsymbol{g} \quad (1)$$

$$\nabla\cdot\boldsymbol{u} = 0 \quad (2)$$

$$\rho c_p\left(\frac{\partial T}{\partial t} + \boldsymbol{u}\cdot\nabla T\right) - \nabla\cdot(k\nabla T) = Q \quad (3)$$

where we have introduced the Boussinesq approximation, $\mathbf{u}$ is the velocity, ρ is density, $\boldsymbol{\tau}$ is stress, $\mathbf{f}$ is body force, β is the coefficient of thermal expansion, T is temperature, T^* is a reference temperature, $\mathbf{g}$ is gravity, c_p is the heat capacity, k is thermal conductivity, and q is a heat source.

A constitutive relation for stress in terms of a viscosity model, pressure and velocity for a generalized Newtonian fluid completes the governing equations in primitive variable form. For free surface applications including thermocapillary surface tension effects the tangential surface shear stress depends on the surface tension gradient and therefore on the surface temperature variation. The remaining (no slip, inflow, outflow) boundary conditions and initial conditions complete the specifications of the problem.

Galerkin Finite Element Formulation

A weighted residual argument applied to the governing equations (1)-(3) together with application of the divergence theorem leads to an integral formulation of the problem with the free surface thermocapillary condition included as a natural boundary condition [2]. Introducing a discretization of C^0 tensor-product stable finite elements [3] in the weak integral statement yields a semidiscrete system of ODE's for the transient problem of the form

$$\begin{aligned}
&\rho\frac{\boldsymbol{M}(\boldsymbol{U}^{n+1}-\boldsymbol{U}^n)}{\Delta t}\\
&+\theta\left[\mu\boldsymbol{A}\boldsymbol{U}^{n+1}+\rho\boldsymbol{s}(\boldsymbol{U}^{n+1})+\boldsymbol{B}\boldsymbol{p}^{n+1}\right]\\
&+(1-\theta)\left[\mu\boldsymbol{A}\boldsymbol{U}^{n}+\rho\boldsymbol{s}(\boldsymbol{U}^{n})+\boldsymbol{B}\boldsymbol{p}^{n}\right]\\
&\quad=\ \theta\boldsymbol{G}^{n+1}+(1-\theta)\boldsymbol{G}^n \qquad (4)
\end{aligned}$$

$$\boldsymbol{B}^T\boldsymbol{U}^{n+1} = \boldsymbol{0} \qquad (5)$$

$$\begin{aligned}
&\frac{\rho c_p\boldsymbol{M}(\boldsymbol{T}^{n+1}-\boldsymbol{T}^n)}{\Delta t}\\
&+\theta\left[\boldsymbol{K}\boldsymbol{T}^{n+1}+\rho c_p\boldsymbol{C}^{n+1}\boldsymbol{T}^{n+1}\right]\\
&+(1-\theta)\left[\boldsymbol{K}\boldsymbol{T}^{n}+\rho c_p\boldsymbol{C}^{n}\boldsymbol{T}^{n}\right]\\
&\quad=\ \theta\boldsymbol{Q}^{n+1}+(1-\theta)\boldsymbol{Q}^n \qquad (6)
\end{aligned}$$

The system is integrated implicitly with respect to time using a Krylov subspace iterative method to solve the Jacobian subsystems of the associated Newton solver.

Parallel Algorithm and Implementation

The Krylov solver requires repeated matrix-vector products and vector dot products that are computed in parallel over the subdomains (one subdomain per processor). Interactions between adjacent subdomains on interprocessor boundaries are communicated using the MPI libraries.

Our algorithms and software for this research are designed to be portable across different architectures. Application stud-

ies are carried out typically on either distributed supercomputer systems such as the Cray T3E at the University of Texas at Austin (UT), the NASA Goddard Cray T3E, and Silicon Graphics Origin systems or on small Beowulf clusters in the CFDLab at UT and the Alaska cluster at Sandia National Laboratory (SNL). The software is designed with parallel scalability in mind [1], and scaled speed-up results are given in Figures 1 and 2 for a typical solution step.

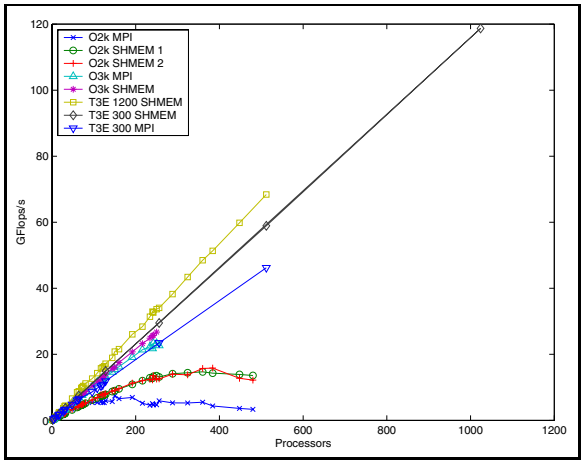

Figure 1: Parallel speedup scaling on Supercomputers

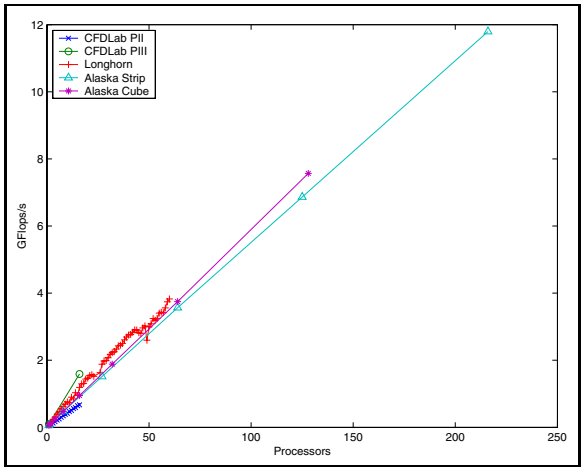

Figure 2: Parallel speedup scaling on Beowulf clusters

Phenomenological Flow Studies

Constitutive Relations

In the present work, we consider generalized Newtonian fluids with constitutive relations of the form

$$\tau = -p\mathbf{I} + \mu\mathbf{D} \tag{7}$$

where p is the pressure, the viscosity $\mu = \mu(s(\mathbf{u}))$, $\mathbf{D} = \mathbf{D}(\mathbf{u})$ denotes the rate of deformation tensor for fluid velocity $\mathbf{u}$,

$$D_{ij} = \frac{1}{2}\left(\frac{\partial u_i}{\partial x_j} + \frac{\partial u_j}{\partial x_i}\right) \tag{8}$$

and s is the shear rate $s(\mathbf{u}) = \sqrt{2D_{ij}D_{ij}}$.

For constant μ, this reduces to the Stokes hypothesis for a Newtonian fluid. We also consider more complex models that are suitable for chemical engineering and biological modeling such as the Powell-Eyring fluid model

$$\mu(s) = \mu_\infty + (\mu_0 - \mu_\infty)\frac{\sinh^{-1}\lambda s}{\lambda s} \tag{9}$$

and the extended Williamson fluid model

$$\mu(s) = \mu_\infty + (\mu_0 - \mu_\infty)\frac{1}{1+(\lambda s)^{2-r}} \tag{10}$$

where the constitutive parameters μ_0, μ_∞, λ, and r satisfy $\mu_0 \geq \mu_\infty \geq 0$, $\lambda > 0$ and $1 \leq r \leq 2$.

A priori error estimates for these fluids in Stokes flow applications have been proved in [4].

Test Case

As a representative test case we consider the backwards facing step in a 3D channel for the Newtonian, Eyring, and Williamson fluid models. Results with this model are shown for a vertical center plane $y = 0$ in Figure 3 for a fluid characterized by parameters $\mu_0 = 1$, $\mu_\infty = .001$, $\lambda = 100$, and $r = 1$.

The results shown in Figure 3 were obtained on a 4096 element grid (generated by Sandia National Laboratory's CUBIT software [5]) using the parallel algorithm described previously and implemented on a Beowulf cluster in the CFDLab. The flow was driven by an imposed normal stress difference between inlet and outlet. Plotted are contours of horizontal velocity component for the results with the Eyring model. Figure 4 shows a comparison of the horizontal velocity component at $x = 1$, $y = 0$ for the three models.

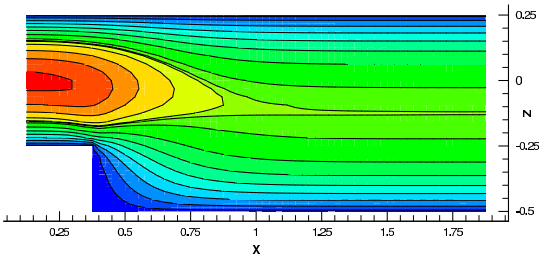

Figure 3: Contours of x velocity at $y = 0$, Eyring Fluid

The CFDLab cluster configuration is comprised of 16 dual Pentium III processor machines operating at 533 MHz with 1 GB of RAM per node. A Sustained performance rate of approximately 115 MFlops/s per processor were achieved in the computationally intensive matrix-vector product and 110 MFlops/s per processor were achieved overall.

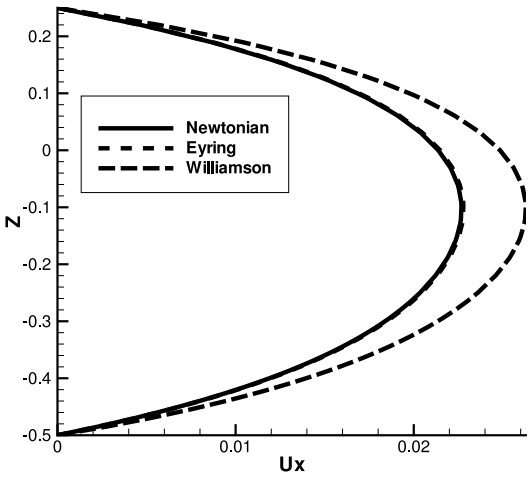

Figure 4: x Velocity Distributions at $x = 1$, $y = 0$

Acknowledgments

This research has been supported in part by ASCI grant B347883 and by the State of Texas Grant 0904 and by grants from Intel and Compaq.

References

[1] Barth, W., Carey, G. F., Kirk, B. and McLay, R., Parallel Distributed Solution Of Viscous Flow With Heat Transfer On Workstation Clusters, in *High Performance Computing '00 Proceedings*, Washington, DC, 2000.

[2] Carey, G. F., McLay, R., Bicken, G. and Barth, B., Parallel Finite Element Solution of 3D Rayleigh-Benard-Marangoni Flows, *IJNMF*, **31**, 1999, 37–52.

[3] Carey, G. F. and Oden, J. T., *Finite Elements, Fluid Mechanics*, volume 6, Prentice Hall, 1986.

[4] Chow, S. and Carey, G., Finite element approximations fo generalized newtonian fluids, Technical report, TICAM, The University of Texas at Austin, 2001.

[5] Cubit mesh generation toolkit, http://endo.sandia.gov/SEACAS/CUBIT/Cubit.html.